



AIAA 2002-0277

**Application of MISDL/KDA Aerodynamics
Prediction Method to Penguin Missile**

D. Lesieutre and M. Dillenius
Nielsen Engineering & Research, Inc.
Mountain View, CA

J.Gjestvang
Kongsberg Defence & Aerospace AS
Kongsberg, Norway

**40th AIAA Aerospace Sciences
Meeting & Exhibit**
14-17 January 2002 / Reno, NV

For permission to copy or republish, contact the copyright owner named on the first page.

For AIAA-held copyright, write to AIAA Permissions Department,
1801 Alexander Bell Drive, Suite 500, Reston, VA, 20191-4344.

APPLICATION OF MISDL/KDA AERODYNAMICS PREDICTION METHOD TO PENGUIN MISSILE

Daniel J. Lesieutre^{*}, Marnix F. E. Dillenius[†]
Nielsen Engineering & Research, Inc.
Mountain View, CA

Jens A. Gjestvang[‡]
Kongsberg Defence & Aerospace AS
Kongsberg, Norway

ABSTRACT

The intermediate-level missile aerodynamic prediction code MISDL has been adapted to handle the particular geometry and operating features of the Kongsberg Defence & Aerospace (KDA) subsonic Penguin MK2 MOD7 missile configuration. The resulting prediction method MISDL/KDA was verified by comparing predicted results to wind tunnel data for a variety of geometric conditions. In addition, the new code has been included in the missile launch simulation method STRLNCH/KDA which is described in AIAA Paper 2002-0278. Because the MISDL/KDA aerodynamic prediction code is called within a 6-DOF simulation, the code had to be computationally efficient. The requirement that the aerodynamic module be called nearly 1500 times in a typical simulation eliminates the consideration of any direct CFD-based approach (at least for now). This paper describes the missile aerodynamics prediction method and presents results that illustrate the unique capabilities of the method.

LIST OF SYMBOLS

C_A, C_X	axial force/ $q_\infty S_R$
C_D	drag force/ $q_\infty S_R$
C_l	rolling moment/ $q_\infty S_R l_R$; positive right wing down
C_m	pitching moment/ $q_\infty S_R l_R$; positive nose up
C_n	yawing moment/ $q_\infty S_R l_R$; positive nose right
C_N, C_Z	normal force/ $q_\infty S_R$
C_Y	side force/ $q_\infty S_R$
l_R	reference length
M_∞	Mach number
S_R	reference area
α_c	included angle of attack, deg
ϕ	roll angle, deg

^{*} Senior Research Engineer, Senior Member AIAA

[†] President, Associate Fellow AIAA

[‡] Project Manager, Member AIAA

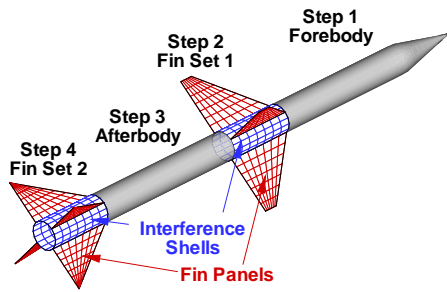
Copyright ©2002 by Nielsen Engineering & Research, Inc.

Published by the American Institute of Aeronautics and Astronautics, Inc. with permission.

BACKGROUND

The development of the intermediate panel method-based aerodynamics prediction method MISDL was started in 1972 under ONR sponsorship for supersonic conditions.² The method was developed further for the Army³ and NASA/LaRC.⁴ It was extended again for the Navy to perform detailed aerodynamic load calculations for a rail-mounted missile on the wing tip of an aircraft for subsonic and supersonic conditions.^{5,6} The extension of the methodology to configurations with noncircular bodies was performed under Air Force sponsorship in the development of a multidisciplinary design optimization method for missiles.⁷ The optimization version of MISDL has been used to design fin planforms with several objectives including minimization of fin hinge moments and maximization of normal force.⁷ A modular version of MISDL has been employed to compute store aerodynamic loads in the comprehensive store trajectory analysis code STRLNCH.⁸

The intermediate-level MISDL code is based on panel methods and other singularity methods enhanced with models for nonlinear vortical effects.^{5-7,9} The body of the missile is modeled by sources/sinks and doublets for volume and angle of attack effects, respectively. The fin sections are modeled by a horseshoe-vortex panel method for subsonic flow. The solution proceeds in a stepwise manner from the body nose to the first fin section, through the first or forward fin section, the length of body from the first fin section trailing edge to the tail (or wing) section, the wing section, and finally the body section aft of the wing section to the base. A schematic of the stepwise procedure and paneling layouts is shown in the following sketch, and body-fixed coordinate systems and sign conventions are shown in Figure 1.



TECHNICAL DESCRIPTION

The aerodynamic prediction methodology in MISDL includes conformal mapping for noncircular body cross sections, and sources/sinks and doublets to model the transformed axisymmetric body. For the fin section, panel methods are employed to compute the lifting surface loadings. Nonlinear effects of body and fin wake vortices are modeled, and fin loads include simplified stall models.

In the application to a body with fins, the body solution is performed first by module VTXCHN.¹⁰⁻¹⁴ The VTXCHN module models circular and noncircular cross section bodies including those with chines. The fin section solution follows with the body-induced effects (perturbation velocities) included in the flow tangency boundary condition applied to the panels on the fins. This procedure is repeated in the case of a canard-tail fin configuration. Effects of vortical wakes from the nose and forward fin section are included in the length of body between the canard and tail section. The solution proceeds in a stepwise manner from the body nose, through the respective fin sections, to the base of the configuration as mentioned earlier.

Descriptions of the body and fin-section models follow.

BODY MODELING METHODOLOGY

The VTXCHN body modeling methodology predicts the aerodynamics of axisymmetric and noncircular body shapes using potential theory and conformal mapping techniques. The calculation proceeds as follows: 1) VTXCHN is used to compute the forebody loads including vortex shedding and tracking, 2) loads within the fin set are calculated including the effects of forebody vorticity, 3) the vorticity shed from the forebody and the forward fin set is included as an initial condition in VTXCHN which tracks and models additional vortices shed from the afterbody (length of body between forward and tail fin sets), and 4) if a second fin set is present, steps 2 and 3 are repeated.

The latest VTXCHN methodology¹⁰⁻¹² is summarized below. VTXCHN is based on analytical engineering-level models providing medium-level aerodynamic fidelity. The methodology embodied in VTXCHN evolved from the vortex shedding modeling schemes developed by Mendenhall et al.^{13,14} The aerodynamic loads acting on bodies with circular and noncircular cross sections, including chine bodies, are computed by VTXCHN under the influence of steady vortex shedding.

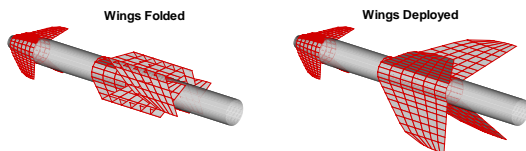
The aerodynamic analysis of a body by VTXCHN comprises conformal mapping,¹⁵ elements of linear and slender body theory, and nonlinear vortical modeling. The analysis proceeds from the nose to the base. The body is sliced into many cross sections which are transformed to corresponding circles in the mapped plane. As a result, an axisymmetric body is created in the mapped space. If the actual body is axisymmetric, this step is omitted. In either case, the axisymmetric body is modeled by 3-D sources/sinks for linear volume effects and by 2-D doublets for linear upwash/sidewash effects.

At the first cross section in the mapped plane, velocity components are computed at points on the transformed (axisymmetric) body and transformed back to the physical plane. If the actual cross section has sharp corners or chine edges, vortices (with strengths determined later) are positioned slightly off the body close to the corner or chine points in the crossflow plane. The circumferential pressure distribution is determined in the physical plane using the compressible Bernoulli expression. For smooth cross sectional contours, the code makes use of the Stratford separation criteria¹⁶ applied to the pressure distribution to determine the separation or vortex shedding points. The locations of the shed vortices are transformed to the mapped plane. The strengths of the shed vortices are related to the imposition of a stagnation condition at the separation points in the mapped plane. The vortices are then tracked aft to the next cross section in the mapped plane. The procedure for the first cross section is repeated. The pressure distribution calculated at the second cross section in the physical plane includes nonlinear effects of the vortices shed from the first cross section. After the pressure distributions have been determined for all cross sections, the aerodynamic forces and moments are obtained by integrating the pressures. At the end of the body, the vortical wake is represented by a cloud of point vortices with known strengths and positions.

FIN SECTION MODELING

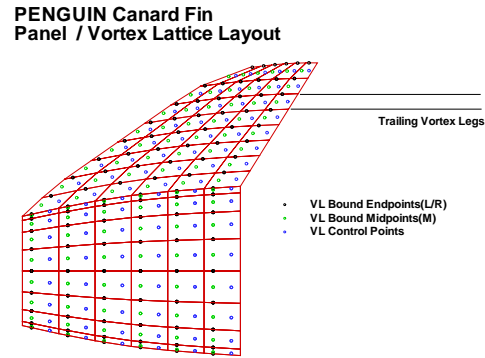
Program SUBDL^{5,7} combined with the VTXCHN module can analyze an arbitrary cross section body with a maximum of two fin sections in subsonic flow. SUBDL and VTXCHN are included as modules in the MISDL/KDA software. The fins may be located off the major planes, and they can be at arbitrary angles to the body surface. The tip chord (if any) need not be parallel to the root chord. The code allows the fins to be in planar, triform, cruciform, or nonconventional (low observable) layouts. The axisymmetric body in the mapped plane (body module VTXCHN) is modeled with subsonic 3-D sources and sinks to account for volume effects, and by 2-D doublets for angle-of-attack effects. The lifting surfaces and the portions of the body spanned by the lifting surfaces, the interference shell, are modeled with planar subsonic lifting panels called horseshoe vortex panels. The strengths of the body and lifting surface singularities are obtained from different sets of linear simultaneous equations based on satisfying the flow tangency condition at a set of discrete aerodynamic control points. The body solution is performed first, and the panel solutions for the canard and tail fins proceed in a stepwise manner. In this process, body on fin interference is included, and fin on body lift carryover is modeled by the interference shells. The fin section modeling procedure is detailed below.

Vortex Lattice Model. The vortex lattice method in MISDL/KDA models the fins and body of a fin section by covering the configuration with a set of discrete panels. As part of the work performed under contract to KDA, the major modifications and extensions made to the MISDL code included the capability to handle folded and partially deployed wings. This involved extending the geometry of the lifting surfaces to allow for changes in dihedral as a function of span. In addition, the root chord of the canard fins was made to conform with the nose meridional shape. In order to accomplish this, the layout of the panels on the fins was modified to handle curvature. These features are shown in the sketch below.



Typically, a vortex lattice panel is composed of a bound vortex segment placed on the $\frac{1}{4}$ chord of each panel and trailing vortices which extend from the bound segment endpoints back to infinity in the axial direction. To model a fin on a nose (or boattail), where the panel

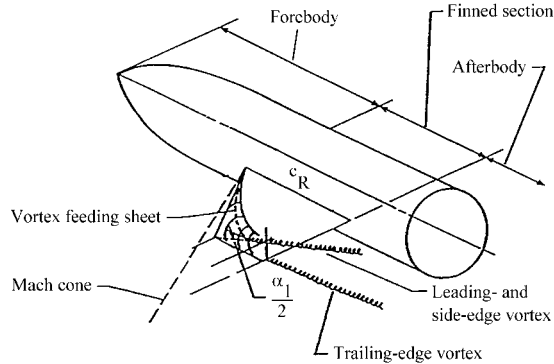
side edges are not in the axial direction, the trailing vortex from each bound segment endpoint must be modeled as a set of bound segments along the panel side edges; at the trailing edge the trailing segments are then assumed to go to infinity in the axial direction. The vortex lattice modeling of fins on a nose is depicted in the following sketch.



The vortex lattice modeling for the Penguin wings has been modified to allow for a fold line and fold angle. For all panels, control points for the vortex lattice system are located midway between the trailing vortex legs at the 75-percent panel chord location. The fins in a fin section are modeled with a set of planar horseshoe vortices. The bound vortex and its trailing vortices are planar. For cases where the wings are folded, a panel edge is forced at the fold line. Therefore, the individual panels are planar inboard and outboard of the fold line. The horseshoe vortices in the interference shell around the body are used only to model the carryover forces between the body and fins (body volume and angle of attack effects are included in the 3-D sources and doublets and conformal mapping procedure). The strengths of the vortex lattice panels are obtained from a set of linear simultaneous equations based on satisfying the flow tangency condition at the control points. This is formulated by enforcing the dot-product of the total velocity and the normal vector at each control point to be zero.

Nonlinear Effects on the Fins. Fins can develop leading- and side-edge separation vorticity as the angle of attack is increased. If the side edge of a given fin is long (similar in length to the root chord, for example), vorticity can be generated along the side edge at angles of attack as low as 5 deg. The leading-edge and side-edge vortices may combine and form a pattern of strong vorticity located above the trailing edge as shown in the sketch which follows. This sketch shows how MISDL models the path of the combined leading- and side-edge vortex by locating it above the fin plane at an angle equal to one-half of the local angle of attack (as

seen by the fin). In the case of a missile, the forward fins may generate leading- and/or side-edge vortices which stream aft along the afterbody and tail section and influence the pressures on those components.



The vortical phenomena along the fin leading- and side-edges are accompanied by augmentation to fin normal force which is nonlinear with angle of attack seen by the fin. This nonlinearity is modeled by calculating the distribution of suction along the leading and side edges. In accordance with an extension⁴ of the Polhamus suction analogy,¹⁷ the suction is converted to normal force in proportion to vortex lift factors. The result is a distribution of nonlinear, additional fin normal force along the leading and the side edge.

A fin stall model is included for more realistic prediction of fin forces above an approximately 10 deg angle of attack. This stall model is based on methods used in the *U.S. Air Force Stability and Control Datcom Handbook*.¹⁸ The fin stall model compares predicted fin section lift coefficients to an empirical/data base maximum section lift coefficient model. This model is a function of the thickness to chord ratio (t/c), the location (x/c) of maximum thickness, the airfoil shape, and the Reynolds number based on local chord. If the predicted lift coefficient for a given section exceeds the stall lift coefficient, the horseshoe vortex strengths determined from the vortex lattice solution are adjusted (reduced) and used in the calculation of the fin forces.

APPLICABLE RANGES

In the MISDL/KDA program, the valid range of Mach numbers is subsonic up to the onset of local supersonic flow (transonic effects). Fin-body angles of attack are generally limited to 30 deg. Angle of roll is arbitrary. Control fins may be deflected up to 20 deg with the upper limit depending on angle of attack; the sum of deflection angle and angle of attack should not exceed

40 deg. Effects of rotational rates and nonuniform flow are included in the methodology. If MISDL/KDA is used to calculate the aerodynamic loads acting on the launched store, the methodology includes perturbation velocities induced by the parent aircraft.

RESULTS

CANARD-TAIL CONFIGURATION

Some results obtained with the original version of MISDL are indicated in Figures 2 and 3 for a supersonic canard-tail wind tunnel model.¹⁹ The longitudinal aerodynamic characteristics calculated with MISDL as a function of angle of attack are compared to wind tunnel data in Figure 2. For this case, the configuration is unrolled and the Mach number is 2.5. Results are shown for zero and for 5 deg canard pitch control. For this canard-control configuration, the essential effect of pitch control is to increase the pitching moment while the normal force is practically unchanged. This behavior is typical for canard control because the effect of the canard wake is to cause a downwash on the tail fins. The prediction agrees well with the data.

In Figure 3 the canard-tail configuration is rolled 26.6 deg, and the canard fins 2 and 4 are differentially deflected 5 deg for right fin up rolling moment. In the upper portion of Figure 3 the Mach number is 1.75; in the lower portion the Mach number is 2.5. Rolling moment only is shown as a function of included angle of attack. Predicted results and experimental data are also shown for tail off showing the direct effect of canard roll control. When the tail fins are attached, the canard fin wakes induce an opposite rolling moment on the tail fins. At low angles of attack, the total rolling moment is near zero. The nonlinear effects of body shed vorticity affects the rolling moment above 6 deg angle of attack. Generally, the rolling moment is predicted well for the cases considered.

PENGUIN CONFIGURATION

Results obtained with the new MISDL/KDA code are compared to low speed wind tunnel data for the Penguin missile²⁰ in Figures 4 and 5. For KDA company proprietary reasons, certain details in the axes can not be shown. In the wind tunnel tests, the Penguin missile was tested in the "X" orientation (rolled 45 deg). For this case, the forces and moments are expressed in the unrolled body coordinate system: C_N is up, C_Y to right.

In Figure 4, the effects of component buildup are shown

in the normal force, pitching moment, drag force and center-of-pressure location over a realistic range in angle of attack. The letter B denotes body alone, BC means canard fins on the body, E/BW means fully deployed wings on the body, E/BWC stands for canard fins and fully deployed wings on the body. In general, the effects of adding components as predicted by MISDL/KDA agree well with the experimental data. For the body alone, it is interesting to note the travel of center-of-pressure from near the nose to a mid-body position as angle of attack increases.

The unique effects of wing deployment are shown in Figure 5. The distinct wing deployment configurations are indicated in the right lower corner of Figure 5 from completely folded A to fully deployed E. It is worth noting that the deployment scenarios not only affect the longitudinal aerodynamic characteristics but the lateral characteristics as well. The latter are particularly difficult to predict. The figure shows normal and side force, pitching, yawing, and rolling moments acting on the complete configuration BWC as a function of angle of attack over a realistic range. In general, the MISDL/KDA code predicts the effects of the various deployed wing configurations reasonably to quite well.

CONCLUSIONS

The intermediate-level missile aerodynamic prediction code MISDL was modified/extended to handle the particular geometry and operating features of the Kongsberg Defence & Aerospace (KDA) subsonic Penguin MK2 MOD7 missile configuration. The resulting prediction method MISDL/KDA is incorporated in the STRLNCH/KDA¹ store trajectory simulation. This paper describes the technical approach and presents comparisons with wind tunnel data including component build-up and partially deployed wings for the Penguin configuration. Overall, MISDL/KDA predicts the aerodynamics of the Penguin well and is computationally efficient allowing its incorporation as the store aerodynamics module in the STRLNCH/KDA simulation program.

ACKNOWLEDGMENT

The work reported herein was performed under contract to Kongsberg Defence & Aerospace AS (KDA) by Nielsen Engineering & Research. The cognizant engineers at KDA are Mr. Jens A. Gjestvang and Mr. Helge Morsund.

REFERENCES

1. Lesieutre, D. J., Dillenius, M. F. E., and Gjestvang, J. A., "Store Separation Simulation of Penguin Missile from Helicopters," AIAA 2002-0278, Jan. 2002.
2. Dillenius, M. F. E. and Nielsen, J. N., "Supersonic Lifting-Surface Computer Program for Cruciform Wing-Body Combinations in Combined Pitch and Sideslip," NEAR TR 74, 1974.
3. Dillenius, M. F. E. and Perkins, S. C., Jr., "Computer Program AMICDM, Aerodynamic Prediction Program for Supersonic Army Type Missile Configurations with Axisymmetric Bodies," U.S. Army Missile Command Technical Report RD-CR-84-15, June 1984.
4. Dillenius, M. F. E., "Program LRCDM2, Improved Aerodynamic Prediction Program for Supersonic Canard-Tail Missiles With Axisymmetric Bodies," NASA CR 3883, Apr. 1985.
5. Lesieutre, D. J., Dillenius, M. F. E., and Whittaker, C. H., "Program SUBSAL and Modified Subsonic Store Separation Program for Calculating NASTRAN Forces Acting on Missiles Attached to Subsonic Aircraft," NAWCWPNS TM 7319, May 1992.
6. Dillenius, M. F. E., Perkins, S. C., Jr., and Lesieutre, D. J., "Modified NWCDM-NSTRN and Supersonic Store Separation Programs for Calculating NASTRAN Forces Acting on Missiles Attached to Supersonic Aircraft," Naval Air Warfare Center Report NWC TP6834, Sep. 1987.
7. Lesieutre, D. J., Dillenius, M. F. E., and Lesieutre, T. O., "Multidisciplinary Design Optimization of Missile Configurations and Fin Planforms for Improved Performance," AIAA 98-4890, Sep. 1998.
8. Dillenius, M. F. E., Love, J. F., Hegedus, M. C., and Lesieutre, D. J., "Program STRLNCH, Simulation of Missile Launch From Maneuvering Aircraft at Subsonic or Supersonic Speeds," NEAR TR 509, Oct. 1996.
9. Dillenius, M. F. E., Lesieutre, D. J., Hegedus, M. C., Perkins, S. C., Jr., Love, J. F., and Lesieutre, T. O., "Engineering-, Intermediate- and High-Level Aerodynamic Prediction Methods and Applications," *Journal of Spacecraft and Rockets*, Vol. 36, No. 5, Sep.-Oct. 1999, pp. 609-620.
10. Albright, A. E., Dixon, C. J., and Hegedus, M. C., "Modification and Validation of Conceptual Design Aerodynamic Prediction Method," NASA CR 4712, Mar. 1996.

11. Hegedus, M., Dillenius, M. F. E., and Love, J., "VTXCHN: Prediction Method For Subsonic Aerodynamics and Vortex Formation on Smooth and Chined Forebodies at High Alpha," AIAA 97-0041, Jan. 1997.
12. Hegedus, M. C., Dillenius, M. F. E., Perkins, S. C., Jr., and Mendenhall, M. R., "Improved Version of the VTXCHN Code," NEAR TR 498, Aug. 1995.
13. Mendenhall, M. R. and Perkins, S. C., Jr., "Prediction of Vortex Shedding from Circular and Non-Circular Bodies in Supersonic Flow," NASA CR 3754, Jan 1984.
14. Mendenhall, M. R. and Lesieutre, D. J., "Prediction of Subsonic Vortex Shedding from Forebodies with Chines," NASA CR 4323, Sep. 1990.
15. Skulsky, R. S., "A Conformal Mapping Method to Predict Low-Speed Aerodynamic Characteristics of Arbitrary Slender Body Re-Entry Shapes," *Journal of Spacecraft*, Vol. 3, No. 2, Feb. 1966, pp. 247-253.
16. Stratford, B. S., "The Prediction of Separation of the Turbulent Boundary Layer," *Journal of Fluid Mechanics*, Vol. 5, 1959, pp. 1-16.
17. Polhamus, E. C., "Prediction of Vortex-Lift Characteristics Based on a Leading-Edge Suction Analogy," *Journal of Aircraft*, Vol. 8, Apr. 1971, pp. 193-199.
18. Hoak, D. E., et al, *USAF Stability and Control DATCOM*, McDonnell Douglas Corp., 1960, revised 1978.
19. Blair, A. B., Jr., Allen, J. M., and Hernandez, G., "Effects of Tail Span on Stability and Control Characteristics of a Canard Controlled Missile at Supersonic Mach Numbers," NASA TP 2157, June 1983.
20. "Penguin MK2 MOD7 Low Speed Wind Tunnel Test Report," Kongsberg Defence & Aerospace AS., Document No. 01TR68072909, Jan. 98.

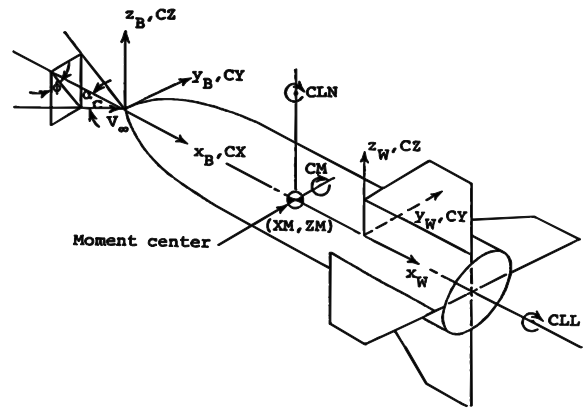


Figure 1.- Coordinate Systems and Force and Moment Convention in MISDL.

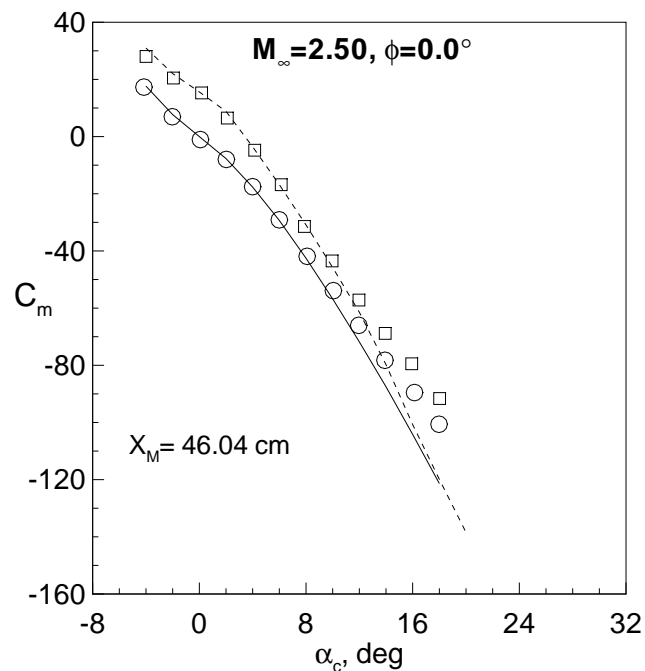
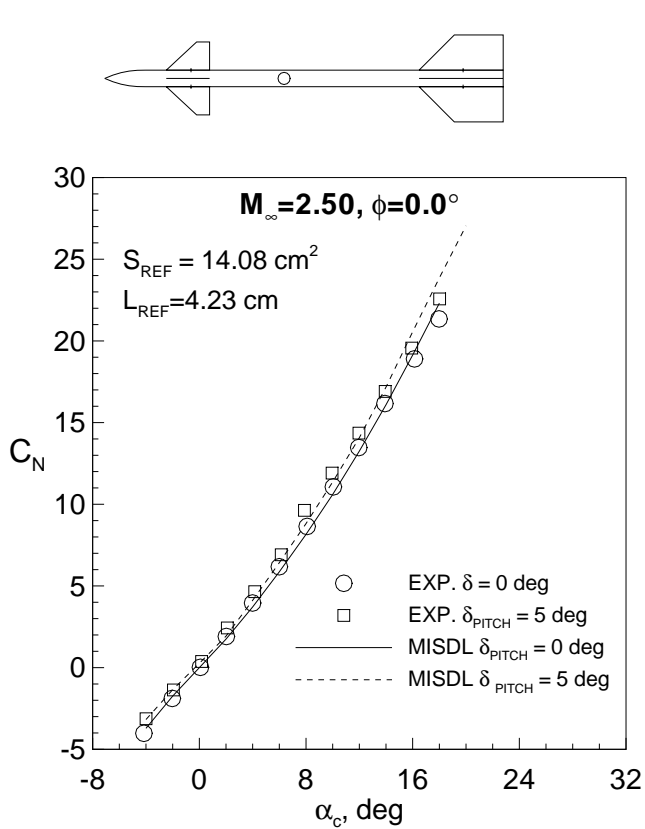


Figure 2.- Comparison of predicted and measured longitudinal aerodynamics of a canard-tail wind tunnel model with canard pitch control; $M_\infty = 2.5, \phi = 0^\circ$.

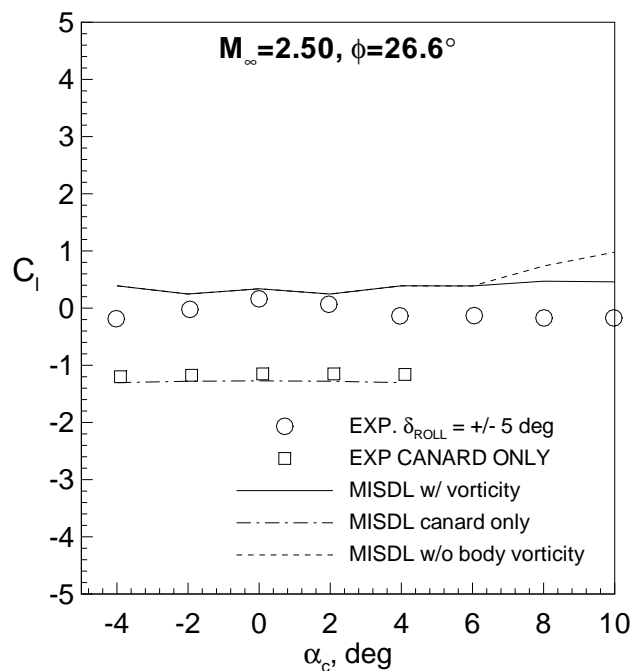
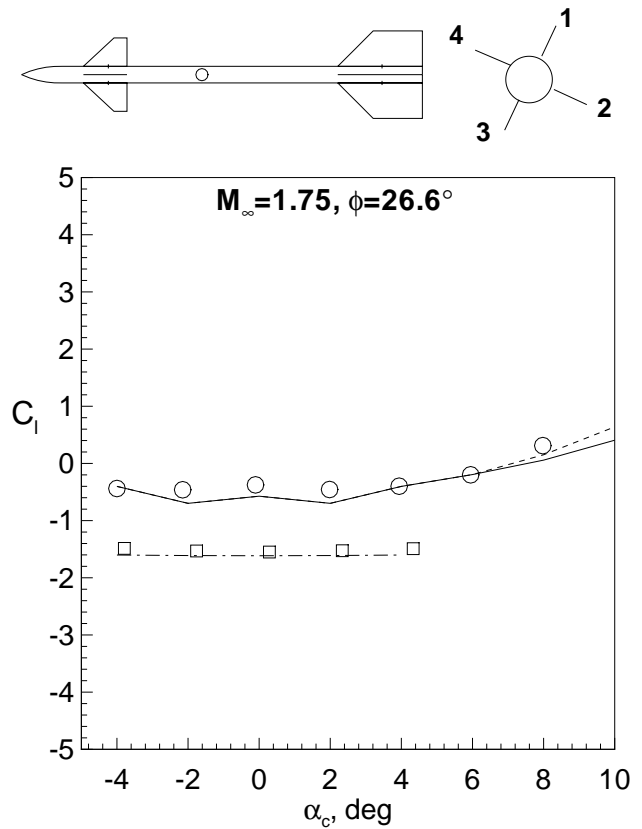


Figure 3.- Comparison of predicted and measured rolling moment of a canard-tail wind tunnel model with canard roll control; fins 2 and 4 differentially deflected; $\phi = 26.6^\circ$.

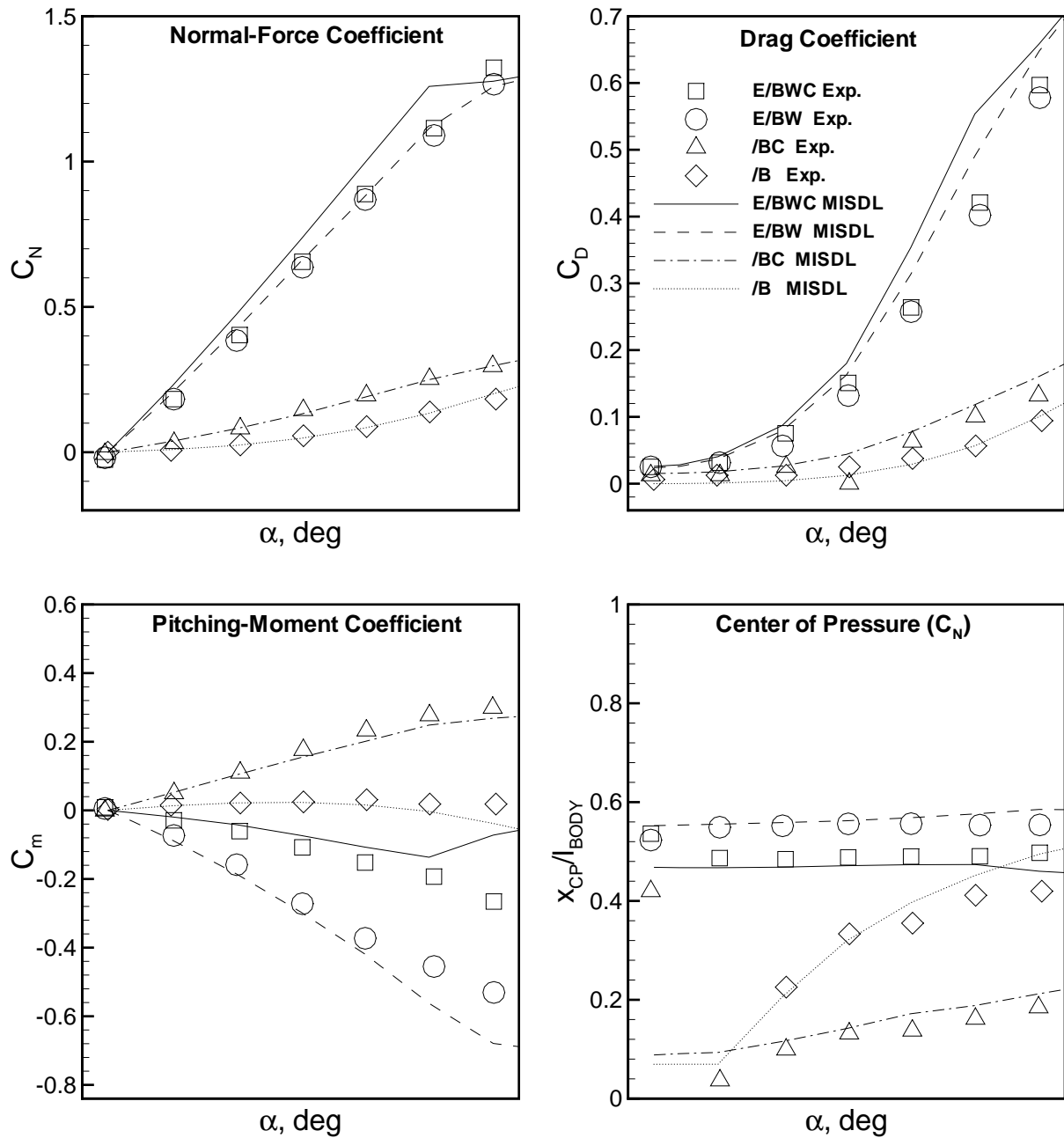
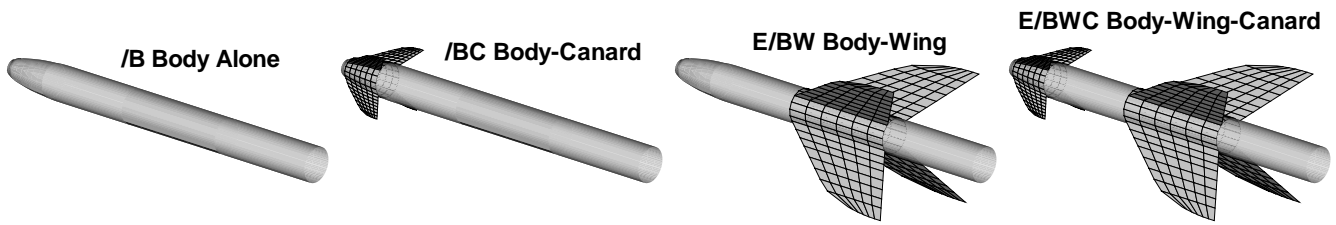


Figure 4.- Comparison of predicted and measured component-buildup aerodynamic characteristics of the Penguin MK2 MOD7 missile configuration.

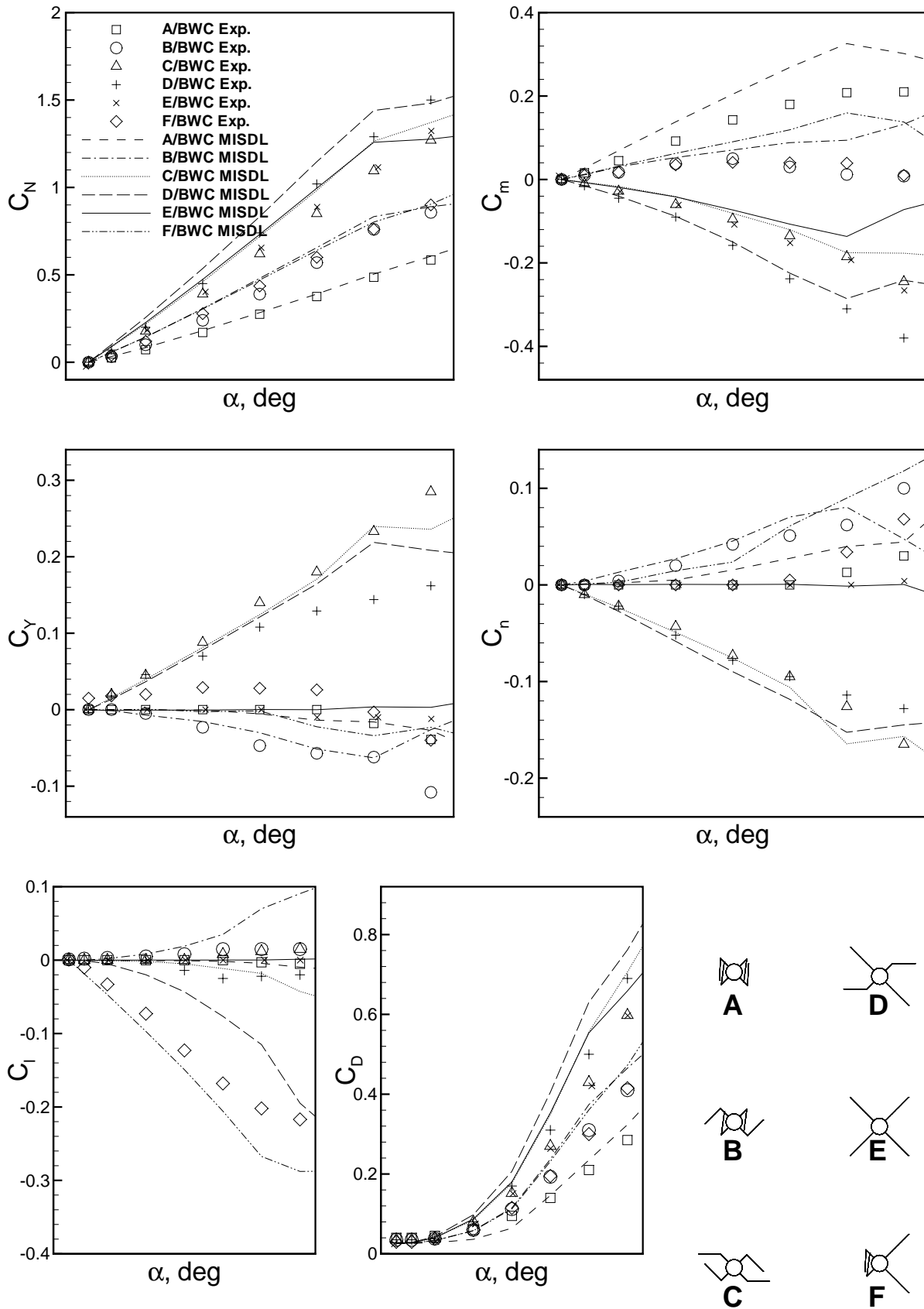


Figure 5.- Comparison of predicted and measured aerodynamic characteristics of the Penguin MK2 MOD7 missile configuration for various wing fold angles.